Journal of Chromatography A 1775 (2026) 466912

Contents lists available at ScienceDirect

Journal of Chromatography A

journal homepage: www.elsevier.com/locate/chroma

Comparing isotherm parameter determination methods for hydrophobic interaction chromatography

Tim Neijenhuis [a], Tomás Cardia e Vale [a], Olivier Le Bussy [b], Geoffroy Geldhof [b], Marieke E. Klijn [a], Marcel Ottens [a,*]

[a] Department of Biotechnology, Delft University of Technology, Delft, the Netherlands
[b] GSK, Rixensart, Belgium

ARTICLE INFO

Keywords:
Mechanistic modeling
Downstream processing
Process development
Preparative chromatography
Linear gradient elution

ABSTRACT

Hydrophobic interaction chromatography (HIC) is a widely used separation method in biopharmaceutical downstream processing. For process development, mechanistic modeling can be used to reduce timelines by simulating protein transport and adsorption during chromatography. Accuracy of the parameters used in the model is essential for successful deployment. This work compares three isotherm parameter determination methods for a simplified linear HIC isotherm: the Parente and Wetlaufer method, the Yamamoto method, and the inverse method. These methods were tested for two proteins, using the same linear gradient elution (LGE) experiments. Accuracy of the obtained parameters was determined via cross-validation using three LGEs. Finally, the obtained parameters were tested for alternative linear gradients with varying initial and final salt concentrations. While all results were comparable, parameters obtained by the inverse method showed the greatest accuracy. This method requires high quality chromatograms, while the other methods only need retention volumes. Therefore, it is less suitable when signal quality is compromised. The Yamamoto method showed similar robustness as the inverse method while outperforming the Parente and Wetlaufer method. Therefore, the Yamamoto method is a good alternative for parameter determination. This comparison offers practical guidance for method selection for isotherm determination, thereby enabling reliable mechanistic modeling of HIC processes.

1. Introduction

Hydrophobic interaction chromatography (HIC) is a separation method widely used at different stages of biopharmaceutical downstream processing [1,2]. It is specifically applied as an orthogonal method for ion exchange chromatography (IEX), as HIC separates based on surface hydrophobicity rather than surface charge [2]. Protein affinity is driven by solvophobic effects, which can be enhanced by anti-chaotropic ions or reduced by chaotropic ions. These effects need to be optimized to establish a robust separation process. Therefore, process development involves an elaborate screening of operation conditions.

To accelerate the design of a chromatographic purification step, in silico tools in combination with high throughput experimentation can be deployed [3–5]. Recently, mechanistic models (MMs) have proven to be valuable by increasing process understanding [6–13]. These models can describe the flow and mass transfer of proteins through a chromatography column. The dynamic adsorption of proteins is captured by adsorption isotherms that describe the equilibrium between the protein concentration in the solid and liquid phase [14]. For HIC, the isotherm developed by Mollerup [15–17] is commonly applied to simulate protein adsorption under varying salt concentrations [18–20]. This isotherm is based on the stochiometric displacement model and uses an activity coefficient to incorporate salt dependency [17]. To apply this isotherm, several parameters require to be determined, which can be done using a set of linear gradient elution (LGE) experiments or batch adsorption experiments. The accuracy of these parameters is essential to ensure successful protein adsorption modeling.

The inverse method (IM) is a common method to estimate isotherm parameters and has been proven to provide accurate simulations for different chromatographic modes [12,21–25]. IM fits the result of the mechanistic model to experimental chromatograms and updates the isotherm parameters to minimize the difference between model and experiment. Therefore, high quality chromatograms of pure components are required for accurate parameter estimation. Alternatively, isotherm

* Corresponding author at: Department of Biotechnology, Delft University of Technology, Van der Maasweg 9, Delft, 2629 HZ, the Netherlands.
E-mail address: M.Ottens@tudelft.nl (M. Ottens).

https://doi.org/10.1016/j.chroma.2026.466912
Received 30 June 2025; Received in revised form 12 March 2026; Accepted 18 March 2026
Available online 19 March 2026

parameters can be estimated from protein retention volumes. The Parente and Wetlaufer (PW) method (non-linear) and the Yamamoto method (linear) are correlations that relate LGE conditions to retention volumes [26,27]. While both methods are developed for IEX, they have been adapted for HIC in recent literature [20,28]. As no iterative simulations are required, using the correlations is computationally more efficient which is beneficial when large datasets are analyzed [29]. However, the correlations only allow determination of the linear part of the isotherm, therefore they can only be used under low loading conditions.

In this work we compare the accuracy of isotherms obtained using IM, PW, and the Yamamoto method using the same LGE experiments. For this we apply the transport dispersive model and the linear part of the isotherm developed by Mollerup to model the adsorption behavior of two proteins under dilute conditions. The model parameters are subsequently validated via cross validation and compared to experimental chromatograms. Quantitative analysis is performed based on differences in peak maxima and peak widths. Finaly, the robustness of the estimated isotherm parameters are tested under alternative salt gradient conditions. Consequently, this work enables informed method selection, enhancing reliability of mechanistic modeling of HIC processes.

2. Methods

2.1. Materials and equipment

The retention experiments were performed on an Äkta pure system (Cytiva, Marlborough, USA), equipped with a prepacked HiTrap Butyl FF 1 mL column (Cytiva, Marlborough, USA) (Appendix A1). All substances were purchased from Sigma-Aldrich (Saint Louis, USA) and buffers were prepared using ultrapure water filtered with the Milli-Q Advantage A10 (Merck Millipore, Burlington, USA). Buffer solutions were prepared using 50 mM sodium phosphate and a range of ammonium sulfate concentrations (2.0 M, 1.5 M, 1.3 M, 1.1 M, 0.8 M and 0 M) which were adjusted to pH 7 using 1 M sodium hydroxide. All buffers were filtered using a 0.2 μm Membrane Disc Filter (Pall corporation, New York, USA) followed by 20 min of sonication.

Chymotrypsinogen A and glucoamylase were purchased from Sigma-Aldrich (Saint Louis, USA). For each experiment, proteins were dissolved in the respective high-salt buffer to reach a concentration of 2 mg/mL, after which the solutions were filtered using a 0.22 μm Whatman Puradisc FP 30 mm (Cytiva, *Marlborough*, USA).

2.2. System and column characterization

To determine relevant system and column properties, a set of pulse experiments with a flowrate of 1 mL/min was performed using a set of nonbinding tracers as described by Schmidt-Traub et al. [30]. Dextran DXT180 (Agilent, Santa Clara, USA) and dextran DXT2000k (Toronto Research Chemicals, Toronto, Canada) were used as penetrating and non-penetrating tracers, respectively. The system dwell volume, describing the volume between the mixing chamber and the column inlet, was determined as described by Keulen et al. [11]. A complete list of the determined properties can be found in Appendix A1 (Table A1).

2.3. Linear gradient elution experiments

A set of LGE experiments were performed with 10, 15, 20, 30 and 40 column volume (CV) gradient lengths with a flowrate of 1 mL/min at room temperature. After equilibration with the high-salt buffer, 200 µL protein solution was injected followed by a 5 CV wash and the start of the salt gradient. Upon reaching the end of the gradient, the column was washed with 10 CV low-salt buffer. During the experiments, UV absorbance was measured at 280 nm and the system was operated using UNICORN version 7.5 software. For the chymotrypsinogen LGEs from 1.5 M to 0 M ammonium sulfate, elution appears to occur in two protein conformations. Therefore, the chromatograms were deconvoluted in Python using two Gaussians that were parameterized by the scipy minimize function.

2.4. Mechanistic model

Simulation of the adsorption behavior of the proteins during the chromatographic experiments was performed using the transport dispersive model (Eq. (1)) combined with the linear driving force (Eq. (2)), as described elsewhere [31,32].

$$\frac{\partial c_p}{\partial t} + F\frac{\partial q}{\partial t} = -u\frac{\partial c_p}{\partial x} + D_L\frac{\partial^2 c_p}{\partial x^2} \tag{1}$$

$$\frac{\partial q}{\partial t} = k_{ov}\left(c_p - c^*_{p,eq}\right), \tag{2}$$

$$k_{ov} = \left[\frac{d_p}{6k_f} + \frac{d_p^2}{60\varepsilon_p D_p}\right]^{-1}. \tag{3}$$

Here, the protein concentration in the liquid and solid phase are denoted as c_p and q, respectively, while $c^*_{p,\,eq}$ is the liquid phase concentration at equilibrium. The phase ratio is defined as $F = (1-\varepsilon_b)/\varepsilon_b$, where ε_b is the bed porosity, u is the interstitial velocity of the mobile phase and D_L is the axial dispersion coefficient calculated using the correlation by Chung and Wen [33]. Dispersion effects in extra-column volumes have been neglected. Time and space are represented by t and x, respectively. The overall mass transfer coefficient (k_{ov}) is defined as the summation of the mass transfer resistance in the film and within the pores. Here, d_p is the particle diameter, D_p is the effective pore diffusivity and ε_p is the intraparticle porosity. The effective pore diffusivity is calculated as

$$D_p = \frac{\varepsilon_p D_f}{\tau}\psi, \tag{4}$$

where D_f is the free diffusivity which is calculated using empirical correlation (Eq. (5)) based on the molecular mass (MW) [34].

$$D_f = 260 * 10^{-11}\left(MW^{-1/3}\right). \tag{5}$$

τ is the tortuosity and ψ the diffusional hindrance parameter determined by Brenner and Gaydos [35]. The film mass transfer coefficient is defined as $k_f = D_f Sh/d_p$ where Sh is the Sherwood number. All equations were solved as described by Keulen et al. (2024) [36].

2.5. Hydrophobic interaction isotherm

In this work, the commonly used HIC isotherm developed by Mollerup [15–17] is used. This isotherm is defined as:

$$\frac{q}{c_p} = K_{eq}\left(\frac{\Lambda}{c}\right)^n\left(1 - \frac{q}{q_{max}}\right)^n \exp\left(K_s c_s + K_p c_p\right), \tag{6}$$

where Λ is the ligand concentration, n is the stochiometric coefficient, c is the molar concentration in the pores, and c_s is the salt concentration. K_{eq}, K_s and K_p are the equilibrium constant, salt and protein interaction parameters, respectively. Finally, q and q_{max} are the current and maximum concentration in the solid phase.

This isotherm allows for some simplifications. Since K_p has been proven to have minor impact under low loading conditions, this parameter can be neglected [20,37,38]. Additionally, assuming that c remains constant [19,28,39] allows for an alternative definition of the equilibrium constant as $K'_{eq} \approx K_{eq}(\Lambda/c)^n$ resulting in the following equation:

$$\frac{q}{c_p} = K'_{eq}\left(1 - \frac{q}{q_{max}}\right)^n \exp\left(K_s c_s\right). \tag{7}$$

Finally, for low loading conditions, it can be assumed that $q \ll q_{max}$, resulting in $(1 - q/q_{max})^n \approx 1$. Applying this to Eq. (7) yields the final form of the linear isotherm used in this study, which is defined as:

$$\frac{q}{c_p} = K'_{eq} \exp(K_s c_s). \tag{8}$$

2.6. Isotherm parameter determination

To apply isotherm Eq. (8), accurate determination of K'_{eq} and K_s is essential. In this work, we will compare three methods which require a set of linear gradient elution (LGE) experiments.

2.6.1. Parente and Wetlaufer

The first approach is based on the Parente and Wetlaufer regression formula, originally developed for ion-exchange chromatography [26]. Chen et al. [40] adapted this formula for HIC:

$$V_{R,g} = \frac{V_G}{-\beta \cdot (c_{s,f} - c_{s,i})} ln\left(1 + V_m \frac{-\beta \cdot (C_{s,f} - C_{s,i})}{V_G} e^{a+\beta \cdot c_{s,i}}\right), \tag{9}$$

where $V_{R,g}$ is the corrected retention volume, V_G is the gradient length, and V_m is the void volume. $C_{s,i}$ and $C_{s,f}$ are the initial and final salt concentrations in the LGE. The corrected retention volume ($V_{R,g}$) was determined as the peak maximum (V_R) and were corrected by:

$$V_{R,g} = V_R - V_m - 0.5V_{inj} - V_{dwell}, \tag{10}$$

where V_{inj} is the injection volume and V_{dwell} the system dwell volume. While Eq. (10) is developed for isocratic elution, the small V_{inj} used in this study allows for adoption of this equation. When applying larger injection volumes, V_{inj} should be removed from Eq. (10). α and β are fitted using the retention volumes at different gradient lengths. The fitted parameters relate to the retention factor by:

$$\ln(k') = \alpha + \beta c_s, \tag{11}$$

as

$$k' = \frac{t_R - t_0}{t_0} = FA_i, \tag{12}$$

where t_R and t_0 are the time of retention and start of the gradient, respectively. A_i is the initial slope of the isotherm, which is equal to Eq. (8). As such, Eq. (9) can be rewritten as follows:

$$V_{R,g} = \frac{V_G}{-K_s (c_{s,f} - c_{s,i})} * \ln\left(1 + V_m F \frac{-K_s (c_{s,f} - c_{s,i})}{V_G} K'_{eq} e^{K_s c_{s,i}}\right). \tag{13}$$

Isotherm parameters K'_{eq} and K_s were fitted using Eq. (13), by scipy.optimize.curve_fit in python.

2.6.2. Yamamoto method

The second method is based on the Yamamoto approach, which was, like the previous method, originally developed for ion-exchange [10,27,41,42]. Recently, Hess et al. adapted this method for the regression of HIC isotherm parameters [41]. This method relates the normalized gradient slope (GH) to the salt concentration at which the peak maximum is observed ($c_{s,R}$) using a linear formula. The normalized gradient slope is defined as follows:

$$GH = g(1 - \epsilon_b) V_{col}, \tag{14}$$

where g is the gradient slope, defined as:

$$g = \frac{c_{s,f} - c_{s,i}}{V_G}, \tag{15}$$

and V_{col} is the total volume of the column. When size exclusion effects are neglected, the normalized gradient length can be related to $c_{s,R}$ by the following linear equation [20]:

$$\ln(-GH) = -K_s c_{s,R} - \ln\left(-K_s K'_{eq}\right) \tag{16}$$

The salt concentration at which the peak maximum is determined by $c_{s,R} = c_{s,i} + gV_{R,g}$. The isotherm parameters are obtained from fitting a linear regression model (sklearn.linear_model.LinearRegression) using $\ln(-GH)$ and $c_{s,R}$ as y and x variables respectively. By combining the regression model and Eq. (16), K_s can be identified as the negative slope of the linear fit, while $K'_{eq} = \exp(-intercept) K_s^{-1}$.

2.6.3. Inverse method

The final approach tested in this study is the inverse method, where the parameters are tuned by running simulations and fitting the results to the experimental data. This is performed by minimizing the sum of squared errors (SSR) calculated by:

$$SSR = \sum_i \sum_{t_0}^{t_{end}} (\hat{c}_i(t) - c_i(t))^2 \tag{17}$$

where $c(t)$ and $\hat{c}(t)$ are protein concentrations at the outlet of the columns at time t determined experimentally and computationally, respectively. This function is minimized using Scipy.minimize with the Nelder-Mead method and initial guesses of 0.01 and 10 for K'_{eq} and K_s respectively. Both the experimental and simulated chromatograms are scaled using a minmax scaler to normalized values between 0 and 1.

2.7. Error calculation

Comparing the accuracy of the isotherm parameters is performed based on retention volume and peak width at 50 % intensity using the scaled chromatograms that result from the mechanistic model. The simulations are performed using a protocol that was nearly identical to the experimental data. As the system dwell volume is not modeled explicitly, the wash prior the gradient start is extended with this volume to a total of 6.025 mL (4.85 mL wash + 1.175 mL dwell volume). The retention volume was determined from the peak maximum, and the absolute error was calculated by subtracting the experimental retention volume from the simulated retention volume. Normalized errors are calculated by dividing the absolute error with the gradient length. Relative peak width is calculated by dividing the modeled peak width by the experimental peak width, both determined at 50 % intensity.

3. Results and discussion

3.1. Linear gradient elution experiments

LGE experiments are required for all three HIC parameter estimation methods. The chromatographic retention of chymotrypsinogen and glucoamylase was measured for 5 gradient lengths (Fig. 1). For both proteins, it was observed that the retention shifts towards the beginning of the gradient. In the chromatogram of chymotrypsinogen at gradient lengths 15 to 40 CV, a shoulder was observed prior to the main peak. This is considered to be a result of a conformational shift, as the high salt concentrations during HIC can cause conformational changes, leading to more than one peak [2,43,44]. When the initial ammonium sulfate concentration was lowered from 1.3 M to 1.1 M, this shoulder was not observed (Supplemental figure S1A). By increasing the initial concentration to 1.5 M, the shoulder moved towards the back of the main peak (Supplemental Figure S1B). This suggests that the dominant conformation shifts to the weaker binding orientation for an increasing salt concentration. Since a distinct peak maximum can be observed for the dominant binding orientation, modeling accuracy should not be compromised. While glucoamylase eluted as a symmetrical peak for all gradient lengths, a small elution curve is observed during the wash (initial isocratic elution). This is most notable for the 40 CV gradient

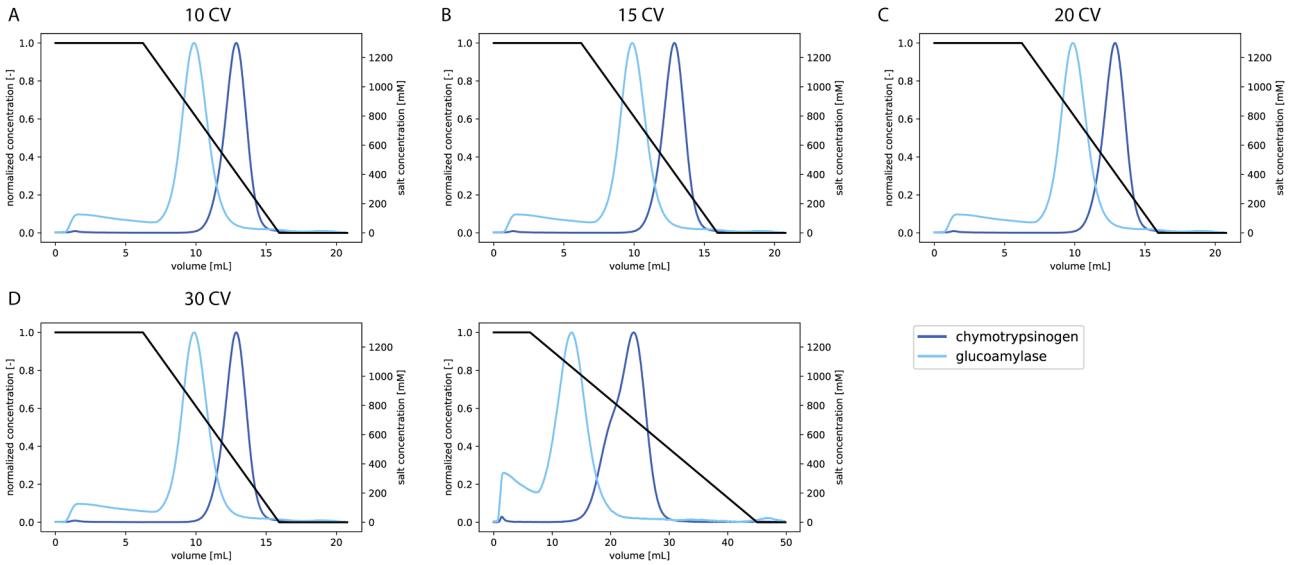

Fig. 1. Superimposed normalized LGE chromatograms for chymotrypsinogen (dark blue) and glucoamylase (light blue) (Hitrap Butyl FF 1 mL, flowrate 1 ml/min) with varying gradient lengths (black).

length where glucoamylase elutes over the greatest volume, resulting in lower peak intensity. As the isocratic elution is far smaller compared to the gradient elution, it is expected to have minimal effect on the quality of the linear isotherm parameters. For both proteins the corrected retention volumes are reported in Table 1.

3.2. Parente and Wetlaufer method

The PW method fits isotherm parameters K'_{eq} and K_s simultaneously to the experimental data. Cross-validation by leaving out individual gradient lengths provided an accurate representation of regression accuracy for data that were not used in the fit (Fig. 2A, Supplemental Figure S2). The cross-validation shows that the retention volumes of gradient lengths 15, 20 and 30 CV are predicted with high accuracy (errors <0.1 mL). For 10 and 40 CV a greater error is observed (errors >0.15 mL and >0.35 mL respectively). The difference in accuracy highlights that the PW method is less accurate when extrapolation is required. For the three intermediate gradient lengths, K'_{eq} values of 0.134 and 0.013 and K_s values of 5.681 and 5.682 chymotrypsinogen and glucoamylase were obtained, respectively.

3.3. Yamamoto method

When using the Yamamoto method, the parameters are obtained using linear regression. Isotherm parameter K_s is directly obtained from the intercept, while K'_{eq} is derived from the slope (Fig. 2B). As observed for the PW method, the Yamamoto method estimates the retention at gradient lengths 15, 20 and 30 CV more accurately compared (errors <0.21 mL) to the gradient lengths at the bounds, especially for the 40 CV LGE, resulting in absolute errors >0.66 mL (Supplemental Figure S3).

Table 1
Corrected experimental retention volumes in mL of chymotrypsinogen and glucoamylase for LGEs with five gradient lengths.

	V_R [mL]	
gradient length [CV]	chymotrypsinogen	glucoamylase
10	6.25	3.24
15	8.25	4.03
20	10.32	4.66
30	13.91	5.7
40	17.34	6.71

For the 15, 20 and 30 CV gradient lengths, fits with R^2 >0.97 were achieved, providing K'_{eq} values of 0.181 and 0.006 and K_s values of 5.350 and 6.488 chymotrypsinogen and glucoamylase, respectively.

3.4. Inverse method

While the previous two methods only require the retention volume, IM uses the full chromatograms as presented in Fig. 3. Because of this, the inverse method does not only optimize for retention volume, but also for peak shape, which comes at the cost of increased computational time (minutes, compared to seconds for the other methods). This method provides average K'_{eq} values of 0.094 and 0.003, and K_s values of 6.137 and 7.331 for chymotrypsinogen and glucoamylase, respectively. As observed for the PW and Yamamoto method, the cross validation shows difficulty to extrapolate gradient lengths, especially for the shorter gradient lengths (Supplemental Figure S4).

3.5. Comparing predictive accuracies

Given the reduced accuracy observed at the shortest (10 CV) and longest (40 CV) gradient lengths, comparisons between methods focus exclusively on the intermediate gradients of 15, 20, and 30 CV. Table 2 presents an overview of the isotherm parameters estimated using the three methods.

For both proteins, IM determines a lower K'_{eq} and a higher K_s compared to the other two methods. A higher K_s indicates a greater salt dependence, resulting in sharper peaks. In contrast to the standard deviation of K'_{eq} which is similar for all methods, the standard deviation for K_s is highest for IM (0.158 and 1.127 for chymotrypsinogen and glucoamylase, respectively), while the other two methods provide more similar deviations (0.054 to 0.073). The high standard deviation is considered to be a result of the extensive fitting effort by IM, which might amplify differences in the data being used.

To determine the actual accuracies of the different parameter combinations, simulations were performed for the 15, 20 and 30 CV gradient length experiments comparing the results to the experimental data (Fig. 4, Supplemental Figure S5). Table 3 shows the average absolute and normalized peak maximum errors as well as the relative peak width for the different parameters. For chymotrypsinogen, peak maxima were predicted with an average error of close to 0.1 mL by all methods. For the peak width, parameters obtained with IM resulted in the best

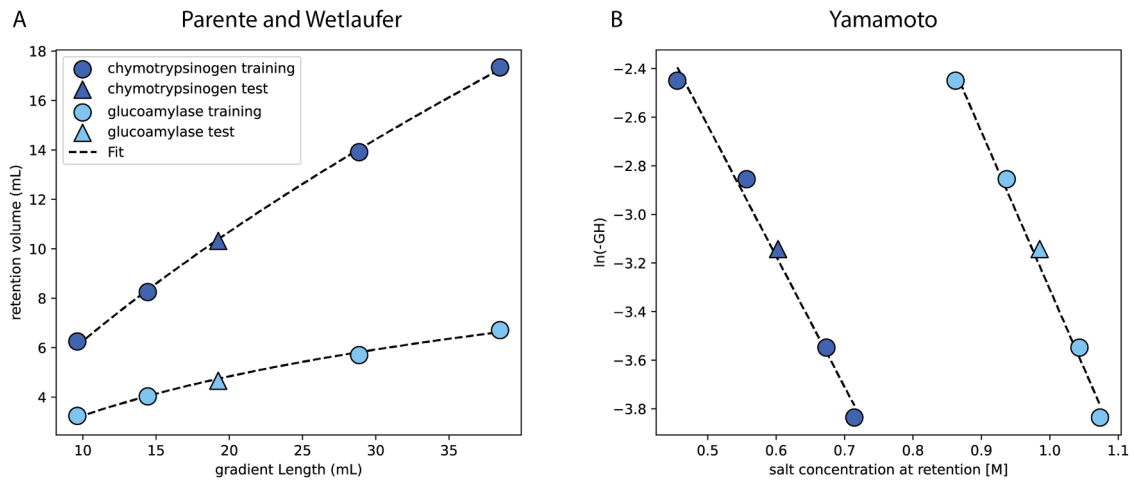

Fig. 2. Isotherm parameter fitting results of chymotrypsinogen (dark) and glucoamylase (light) for the 20 CV gradient length as test (triangle) and the remaining gradient lengths as fitting data (circles). A) shows the Parente and Wetlaufer method results with gradient length on the x-axis and retention volume on the y-axis. B) shows the Yamamoto method results with salt concentration of the peak maximum on the x-axis and the natural log of the normalized gradient slope on the y-axis.

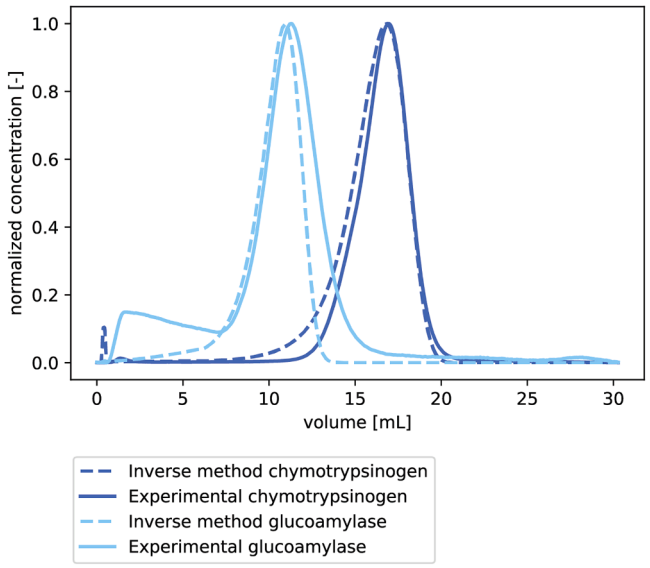

Fig. 3. Superimposed normalized inverse method results of chymotrypsinogen (dark) and glucoamylase (light) for the 20 CV gradient length test. The dashed line depicts the model results while the continuous line shows the experimental chromatogram.

Table 2
Isotherm parameters obtained from cross-validation excluding 15, 20 and 30 CV gradient lengths iteratively.

	K'_{eq} [-]	K_s [M^{-1}]
Chymotrypsinogen		
PW	0.134±0.006	5.681±0.054
Yamamoto method	0.181±0.010	5.35±0.058
IM	0.094±0.011	6.137±0.158
Glucoamylase		
PW	0.013±0.001	5.682±0.073
Yamamoto method	0.006±0.001	6.488±0.063
IM	0.003±0.000	7.331±1.127

agreement with the experimental data (relative peak width of 1.018). This is to be expected since this method considers chromatogram shape during the fitting. Simulations using the parameters obtained from the PW and Yamamoto method resulted in broader peaks (relative width of 1.095 and 1.164, respectively), which can be attributed to the lower K_s and higher K'_{eq} compared to the IM.

Simulations of glucoamylase retention showed to be more challenging, resulting in higher absolute errors compared to chymotrypsinogen. Especially parameters estimated using PW led to an average retention offset of 1.1 mL, while the Yamamoto method and IM achieved offsets below 0.4 mL. This might be attributed to the fact that glucoamylase elutes early in the gradient, even displaying minor isocratic elution. Interestingly, while IM yielded the most accurate retention times overall, it also produced the largest deviations in peak width. As shown in Fig. 4B, the simulations accurately captured the initial slope of the chromatogram but predicted a too steep descent after reaching the peak maximum.

To verify whether the early elution of glucoamylase limits the accuracy of the different methods, gradients starting at 1.5 M ammonium sulfate were used for parameter determination (Supplemental Table S1). These parameters were subsequently used to predict the behavior of glucoamylase at a gradient running from 1.3 M to 0 M ammonium sulfate (Table 3). For the PW parameters, the simulation accuracy was significantly improved to an average retention error of 0.54 mL. For the Yamamoto and inverse method, accuracy was slightly reduced to an average error of 0.44 mL, while the normalized error remained constant.

3.6. Predicting alternative salt gradients

To assess the quality of the isotherm and the parameters, the obtained parameter sets were tested for other salt concentrations. For chymotrypsinogen, two additional gradients were measured starting at 1.1 M and 1.5 M ammonium sulfate, both reaching a final concentration of 0 M. The additional salt gradients for glucoamylase were measured at 1.5 M to 0 M and 2.0 to 0.8 M ammonium sulfate (Fig. 5, Table 4). Simulations were performed using the parameters determined based on the 1.3 M to 0 M gradients for chymotrypsinogen, while for glucoamylase the gradients starting at 1.5 M were used.

For all three methods, retention could be predicted with high accuracy, resulting in an average retention offset <0.44 mL. While the parameters obtained from the Yamamoto method resulted in simulated chromatograms with the smallest error in peak maxima (0.03 to 0.33 mL), the relative widths are highest (1.16 to 1.28). Simulations using the parameters obtained from the inverse method result in chromatograms with peak widths closest to the experimental peaks (1.03 to 1.12 relative widths). Peak widths for chymotrypsinogen starting at 1.5 M ammonium sulfate were estimated with the greatest deviation from the experimental data (1.12 to 1.28 relative widths). For these conditions, the

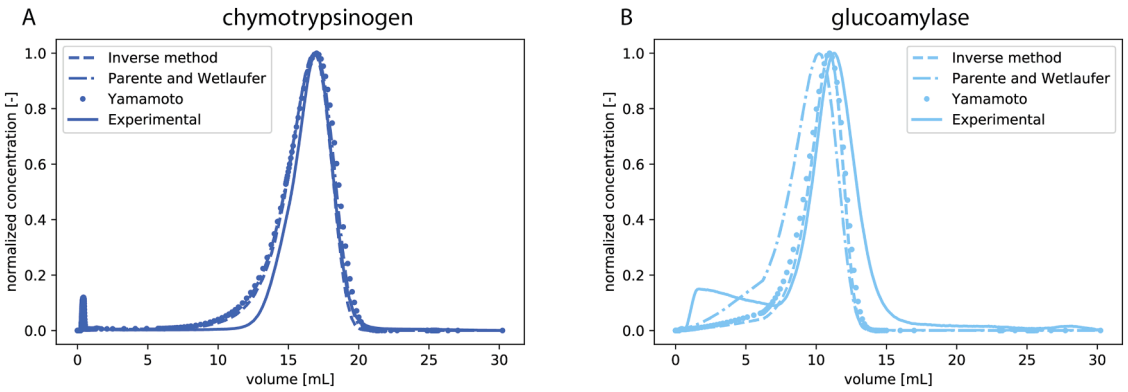

Fig. 4. Normalized modeled and experimental chromatogram of chymotrypsinogen (A) and glucoamylase (B) with a 20 CV linear gradient starting at 1.3 M ammonium sulfate.

Table 3
Average quantitative modeling accuracy measures for the different parameter sets*.

	chymotrypsinogen	glucoamylase	glucoamylase*
Absolute retention error [mL]			
PW	0.119	1.096	0.539
Yamamoto method	0.095	0.389	0.440
IM	0.119	0.273	0.440
Normalized retention error [-]			
PW	0.0056	0.0525	0.0267
Yamamoto method	0.0043	0.0192	0.0211
IM	0.0057	0.0154	0.0143
Relative peak width [-]			
PW	1.095	1.084	0.946
Yamamoto method	1.164	0.917	1.023
IM	1.018	0.803	0.938

* parameters determined using the 1.5 M to 0 M ammonium sulfate LGEs.

chymotrypsinogen peak was deconvoluted from the experimental data using two gaussians (Supplemental Figure S6). Therefore, the chromatogram (Fig. 5B) is an estimation of the elution which might actually

Table 4
Average quantitative modeling accuracies for the alternative LGEs.

	chymotrypsinogen		glucoamylase	
Ammonium sulfate [M]	1.1 – 0	1.5 - 0	1.5 - 0	2.0 – 0.8
Absolute retention error [mL]				
PW	0.357	0.431	0.070	0.143
Yamamoto method	0.206	0.328	0.031	0.077
IM	0.311	0.431	0.206	0.288
Normalized retention error [-]				
PW	0.0163	0.0216	0.0039	0.0070
Yamamoto method	0.0103	0.0156	0.0014	0.0028
IM	0.0162	0.0216	0.0080	0.0128
Relative peak width [-]				
PW	1.111	1.207	1.066	1.074
Yamamoto method	1.179	1.283	1.164	1.171
IM	1.027	1.116	1.055	1.070

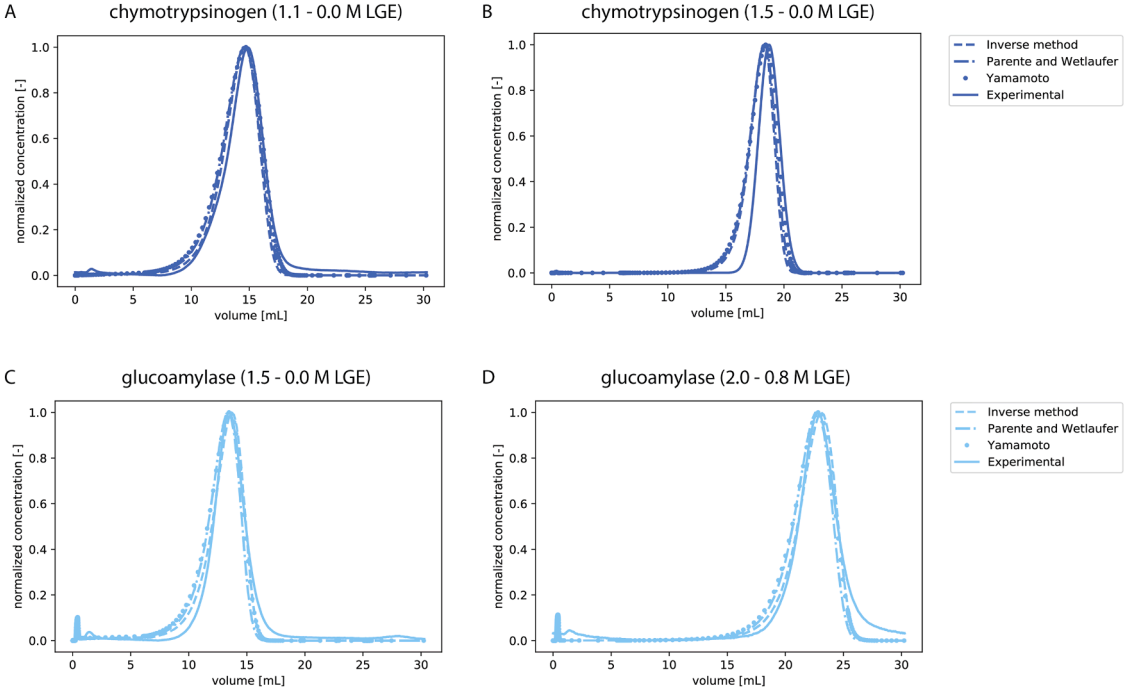

Fig. 5. Normalized predicted (dashed, dash-doted, and dotted) and experimental (continuous) chromatograms of chymotrypsinogen (dark) and glucoamylase (light) for the 20 CV LGE at alternative buffer compositions. A) and B) show chymotrypsinogen ammonium sulfate LGEs 1.1 M to 0 M and 1.5 M to 0 M, respectively. C) and D) show glucoamylase LGEs from 1.5 M to 0 M and 2.0 M to 0.8 M, respectively.

occur less symmetrical, as was observed for chymotrypsinogen when starting the LGE at 1.1 M ammonium sulfate (Fig. 5A).

Overall, all three methods provided parameters to model the retention of both proteins accurately. Even though the two correlation methods only use peak maxima information, the peak shape can be predicted with a maximum over estimation of 30 %. Therefore, for the simplified Mollerup isotherm, the correlations are good alternatives to the more computationally expensive inverse method. This is useful when data quality is compromised, as was seen for the LGE starting at 1.5 M ammonium sulfate for the elution of chymotrypsinogen. Comparing the two correlations, the Yamamoto method provides the most accurate peak maxima for the two proteins, while the PW method results in more accurate peak widths. Additionally, the linear representation of the Yamamoto method showed to be more robust compared to the PW method for the early elution of glucoamylase for the 1.3 M to 0 M ammonium sulfate LGE. This is likely due to the correction term present in the PW method. For elution later in the gradient, this correction factor becomes neglectable, resulting in more similar solutions of the PW and Yamamoto methods.

It is important to note that there are alternative correlations for D_p (Eq. (4)) and D_f (Eq. (5)), which might result in more accurate simulations for other resins or proteins [45–49]. Additionally, the linear isotherm used in this study (Eq. (8)) is only valid for low loading conditions. Therefore, it cannot be used for simulating the high loading conditions which require the non-linear form as shown in Eqn 6 Nevertheless, the linear isotherm is still useful for early process design, to scout for promising conditions, or for low concentration contaminants such as host cell proteins.

4. Conclusion

In this study, we have compared the Parente and Wetlaufer method, the Yamamoto method, and the inverse method to obtain isotherm parameters for a simplified Mollerup isotherm for HIC. The different methods were applied using five LGE experiments (10, 15, 20, 30, and 40 CV gradient lengths) for chymotrypsinogen and glucoamylase. While the different methods estimated parameters within the same order of magnitudes, the early elution of glucoamylase resulted in systemic under prediction using the parameters estimated by the PW method, which was not observed for the other methods. Overall, the inverse method performed best, but was also most computationally expensive, and required high-quality chromatograms. Therefore, the Yamamoto method is a good alternative for the inverse method when data quality is compromised, or computational resources are limited. This comparison offers practical guidance for isotherm determination method selection, thereby enabling reliable mechanistic modeling of HIC processes.

Data availability

Research data are not shared.

CRediT authorship contribution statement

Tim Neijenhuis: Writing – review & editing, Writing – original draft, Visualization, Validation, Methodology, Investigation, Data curation, Conceptualization. **Tomás Cardia e Vale:** Validation, Methodology, Investigation. **Olivier Le Bussy:** Writing – review & editing, Supervision. **Geoffroy Geldhof:** Writing – review & editing, Supervision. **Marieke E. Klijn:** Writing – review & editing, Supervision. **Marcel Ottens:** Writing – review & editing, Supervision, Funding acquisition, Conceptualization.

Declaration of competing interest

Geoffroy Geldhof and Olivier Le Bussy are employees of the GSK group of companies. The remaining authors declare no conflicts of interest.

Acknowledgements

This work was partly financed from PSS-allowance for Top consortiums for Knowledge and Innovation (TKI) of the ministry of Economic Affairs and partly sponsored by GlaxoSmithKline Biologicals S.A. under cooperative research and development agreement between GlaxoSmithKline Biologicals S.A. (Belgium) and the Technical University of Delft (The Netherlands). The authors thank the colleagues from GSK and Technical University of Delft for their valuable input.

Supplementary materials

Supplementary material associated with this article can be found, in the online version, at doi:10.1016/j.chroma.2026.466912.

Appendix 1

Table A1
system and column parameters.

Parameter	Value	Unit
Column diameter	0.70	cm
Column height	2.50	cm
Particle size	90	μm
Total porosity (ε_t)	0.914	-
Extraparticle porosity (ε_b)	0.336	-
Intraparticle porosity (ε_p)	0.870	-
Void volume (V_m)	0.323	mL
System dead volume	0.281	mL
System dwell volume	1.175	mL

References

[1] K.O. Eriksson, Hydrophobic Interaction Chromatography, Elsevier Ltd., 2018, https://doi.org/10.1016/B978-0-08-100623-8.00019-0.

[2] B.C.S. To, A.M. Lenhoff, Hydrophobic interaction chromatography of proteins. I. The effects of protein and adsorbent properties on retention and recovery, J. Chromatogr. A 1141 (2007) 191–205, https://doi.org/10.1016/j.chroma.2006.12.020.

[3] D. Keulen, G. Geldhof, O. Le Bussy, M. Pabst, M. Ottens, Recent advances to accelerate purification process development: a review with a focus on vaccines, J. Chromatogr. A 1676 (2022) 463195, https://doi.org/10.1016/j.chroma.2022.463195.

[4] A.T. Hanke, M. Ottens, Purifying biopharmaceuticals: knowledge-based chromatographic process development, Trends Biotechnol. 32 (2014) 210–220, https://doi.org/10.1016/j.tibtech.2014.02.001.

[5] F. Wittkopp, J. Welsh, R. Todd, A. Staby, D. Roush, J. Lyall, S. Karkov, S. Hunt, J. Griesbach, M.O. Bertran, D. Babi, Current state of implementation of in silico tools in the biopharmaceutical industry—Proceedings of the 5th modeling workshop, Biotechnol. Bioeng. (2024) 2952–2973, https://doi.org/10.1002/bit.28768.

[6] B.K. Nfor, T. Ahamed, M.W.H. Pinkse, L.A.M. van der Wielen, P.D.E.M. Verhaert, G.W.K. van Dedem, M.H.M. Eppink, E.J.A.X. van de Sandt, M. Ottens, Multi-dimensional fractionation and characterization of crude protein mixtures: toward establishment of a database of protein purification process development parameters, Biotechnol. Bioeng. 109 (2012) 3070–3083, https://doi.org/10.1002/bit.24576.

[7] S.M. Pirrung, C. Berends, A.H. Backx, R.F.W.C. van Beckhoven, M.H.M. Eppink, M. Ottens, Model-based optimization of integrated purification sequences for biopharmaceuticals, Chem. Engin. Sci.: X 3 (2019) 100025, https://doi.org/10.1016/j.cesx.2019.100025.

[8] N. Vecchiarello, S.M. Timmick, C. Goodwine, L.E. Crowell, K.R. Love, J.C. Love, S. M. Cramer, A combined screening and in silico strategy for the rapid design of integrated downstream processes for process and product-related impurity removal, Biotechnol. Bioeng. 116 (2019) 2178–2190, https://doi.org/10.1002/bit.27018.

[9] D. Keulen, M. Apostolidi, G. Geldhof, O.Le Bussy, M. Pabst, M. Ottens, Comparing in silico flowsheet optimization strategies in biopharmaceutical downstream processes, Biotechnol. Prog. (2024) 1–16, https://doi.org/10.1002/btpr.3514.

[10] D. Saleh, G. Wang, B. Müller, F. Rischawy, S. Kluters, J. Studts, J. Hubbuch, Straightforward method for calibration of mechanistic cation exchange chromatography models for industrial applications, Biotechnol. Prog. 36 (2020) 1–12, https://doi.org/10.1002/btpr.2984.

[11] D. Keulen, T. Neijenhuis, A. Lazopoulou, R. Disela, G. Geldhof, O.Le Bussy, M. E. Klijn, M. Ottens, From protein structure to an optimized chromatographic capture step using multiscale modeling, Biotechnol. Prog. (2024) 1–26, https://doi.org/10.1002/btpr.3505.

[12] V. Kumar, A.M. Lenhoff, Mechanistic modeling of preparative column chromatography for biotherapeutics, Annu Rev. Chem. Biomol. Eng. 11 (2020) 235–255, https://doi.org/10.1146/annurev-chembioeng-102419-125430.

[13] L.K. Shekhawat, A. Tiwari, S. Yamamoto, A.S. Rathore, An accelerated approach for mechanistic model based prediction of linear gradient elution ion-exchange chromatography of proteins, J. Chromatogr. A 1680 (2022) 463423, https://doi.org/10.1016/j.chroma.2022.463423.

[14] M.A. Al-Ghouti, D.A. Da'ana, Guidelines for the use and interpretation of adsorption isotherm models: a review, J. Hazard. Mater. 393 (2020) 122383, https://doi.org/10.1016/j.jhazmat.2020.122383.

[15] J.M. Mollerup, Applied thermodynamics: a new frontier for biotechnology, Fluid. Phase Equilib. 241 (2006) 205–215, https://doi.org/10.1016/j.fluid.2005.12.037.

[16] J.M. Mollerup, The thermodynamic principles of ligand binding in chromatography and biology, J. Biotechnol. 132 (2007) 187–195, https://doi.org/10.1016/j.jbiotec.2007.05.036.

[17] J.M. Mollerup, A review of the thermodynamics of protein association to ligands, protein adsorption, and adsorption isotherms, Chem. Eng. Technol. 31 (2008) 864–874, https://doi.org/10.1002/ceat.200800082.

[18] E. Lietta, A. Pieri, A.G. Cardillo, M. Vanni, R. Pisano, A.A. Barresi, An experimental and modeling combined approach in preparative hydrophobic interaction chromatography, Processes 10 (2022), https://doi.org/10.3390/pr10051027.

[19] S. Andris, J. Hubbuch, Modeling of hydrophobic interaction chromatography for the separation of antibody-drug conjugates and its application towards quality by design, J. Biotechnol. 317 (2020) 48–58, https://doi.org/10.1016/j.jbiotec.2020.04.018.

[20] Y.X. Yang, Y.C. Chen, S.J. Yao, D.Q. Lin, Parameter-by-parameter estimation method for adsorption isotherm in hydrophobic interaction chromatography, J. Chromatogr. A 1716 (2024) 464638, https://doi.org/10.1016/j.chroma.2024.464638.

[21] T. Hahn, P. Baumann, T. Huuk, V. Heuveline, J. Hubbuch, UV absorption-based inverse modeling of protein chromatography, Eng. Life Sci. 16 (2016) 99–106, https://doi.org/10.1002/elsc.201400247.

[22] A. Osberghaus, S. Hepbildikler, S. Nath, M. Haindl, E. von Lieres, J. Hubbuch, Determination of parameters for the steric mass action model-A comparison between two approaches, J. Chromatogr. A 1233 (2012) 54–65, https://doi.org/10.1016/j.chroma.2012.02.004.

[23] A. Osberghaus, S. Hepbildikler, S. Nath, M. Haindl, E. von Lieres, J. Hubbuch, Optimizing a chromatographic three component separation: a comparison of mechanistic and empiric modeling approaches, J. Chromatogr. A 1237 (2012) 86–95, https://doi.org/10.1016/j.chroma.2012.03.029.

[24] S.V. Rajagopala, P. Sikorski, A. Kumar, R. Mosca, J. Vlasblom, R. Arnold, J. Franca-Koh, S.B. Pakala, S. Phanse, A. Ceol, R. Häuser, G. Siszler, S. Wuchty, A. Emili, M. Babu, P. Aloy, R. Pieper, P. Uetz, The binary protein-protein interaction landscape of *Escherichia coli*, Nat. Biotechnol. 32 (2014) 285–290, https://doi.org/10.1038/nbt.2831.

[25] V. Kumar, S. Leweke, E. von Lieres, A.S. Rathore, Mechanistic modeling of ion-exchange process chromatography of charge variants of monoclonal antibody products, J. Chromatogr. A 1426 (2015) 140–153, https://doi.org/10.1016/j.chroma.2015.11.062.

[26] E.S. Parente, D.B. Wetlaufer, Relationship between isocratic and gradient retention times in the high-performance ion-exchange chromatography of proteins. Theory and experiment, J. Chromatogr. A 355 (1986) 29–40, https://doi.org/10.1016/S0021-9673(01)97301-7.

[27] S. Yamamoto, Electrostatic interaction chromatography process for protein separations: impact of engineering analysis of biorecognition mechanism on process optimization, Chem. Eng. Technol. 28 (2005) 1387–1393, https://doi.org/10.1002/ceat.200500199.

[28] A.T. Hanke, E. Tsintavi, M.del P. Ramirez Vazquez, L.A.M. van der Wielen, P.D.E. M. Verhaert, M.H.M. Eppink, E.J.A.X. van de Sandt, M. Ottens, 3D-liquid chromatography as a complex mixture characterization tool for knowledge-based downstream process development, Biotechnol. Prog. 32 (2016) 1283–1291, https://doi.org/10.1002/btpr.2320.

[29] R. Disela, D. Keulen, E. Fotou, T. Neijenhuis, O.Le Bussy, G. Geldhof, M. Pabst, M. Ottens, Proteomics-based method to comprehensively model the removal of host cell protein impurities, Biotechnol. Prog. (2024), https://doi.org/10.1002/btpr.3494.

[30] H. Schmidt-Traub, M. Schulte, A. Seidel-Morgenstern, Preparative Chromatography, 3rd ed., John Wiley & Sons., 2020 https://doi.org/10.1002/9783527816347.

[31] B.K. Nfor, D.S. Zuluaga, P.J.T. Verheijen, P.D.E.M. Verhaert, L.A.M. van der Wielen, M. Ottens, Model-based rational strategy for chromatographic resin selection, Biotechnol. Prog. 27 (2011) 1629–1643, https://doi.org/10.1002/btpr.691.

[32] H. Schmidt-Traub, M. Schulte, A. Seidel-Morgenstern, Preparative Chromatography, 3rd ed., John Wiley & Sons., 2020 https://doi.org/10.1002/9783527816347.

[33] S.F. Chung, C.Y. Wen, Longitudinal dispersion of liquid flowing through fixed and fluidized beds, AIChE J. 14 (1968) 857–866, https://doi.org/10.1002/aic.690140608.

[34] L. Hagel, Protein purification- 3 - gel filtration: size exclusion chromatography, Prot. Purific. (2011) 51–91.

[35] H. Brenner, L.J. Gaydos, The constrained brownian movement of spherical particles in cylindrical pores of comparable radius, J. Colloid. Interface Sci. 58 (1977) 312–356, https://doi.org/10.1016/0021-9797(77)90147-3.

[36] D. Keulen, E. van der Hagen, G. Geldhof, O.Le Bussy, M. Pabst, M. Ottens, Using artificial neural networks to accelerate flowsheet optimization for downstream process development, Biotechnol. Bioeng. 121 (2024) 2318–2331, https://doi.org/10.1002/bit.28454.

[37] B.K. Nfor, M. Noverraz, S. Chilamkurthi, P.D.E.M. Verhaert, L.A.M. van der Wielen, M. Ottens, High-throughput isotherm determination and thermodynamic modeling of protein adsorption on mixed mode adsorbents, J. Chromatogr. A 1217 (2010) 6829–6850, https://doi.org/10.1016/j.chroma.2010.07.069.

[38] R.W. Deitcher, J.E. Rome, P.A. Gildea, J.P. O'Connell, E.J. Fernandez, A new thermodynamic model describes the effects of ligand density and type, salt concentration and protein species in hydrophobic interaction chromatography, J. Chromatogr. A 1217 (2010) 199–208, https://doi.org/10.1016/j.chroma.2009.07.068.

[39] R. Hess, D. Yun, D. Saleh, T. Briskot, J.H. Grosch, G. Wang, T. Schwab, J. Hubbuch, Standardized method for mechanistic modeling of multimodal anion exchange chromatography in flow through operation, J. Chromatogr. A 1690 (2023) 463789, https://doi.org/10.1016/j.chroma.2023.463789.

[40] J. Chen, T. Yang, S.M. Cramer, Prediction of protein retention times in gradient hydrophobic interaction chromatographic systems, J. Chromatogr. A 1177 (2008) 207–214, https://doi.org/10.1016/j.chroma.2007.11.003.

[41] M. Rüdt, F. Gillet, S. Heege, J. Hitzler, B. Kalbfuss, B. Guélat, Combined Yamamoto approach for simultaneous estimation of adsorption isotherm and kinetic parameters in ion-exchange chromatography, J. Chromatogr. A 1413 (2015) 68–76, https://doi.org/10.1016/j.chroma.2015.08.025.

[42] S. Yamamoto, M. Nomura, Y. Sano, Adsorption chromatography of proteins: determination of optimum conditions, AIChE J. 33 (1987) 1426–1434, https://doi.org/10.1002/aic.690330903.

[43] R. Ueberbacher, E. Haimer, R. Hahn, A. Jungbauer, Hydrophobic interaction chromatography of proteins. V. Quantitative assessment of conformational changes, J. Chromatogr. A 1198–1199 (2008) 154–163, https://doi.org/10.1016/j.chroma.2008.05.062.

[44] B. Beyer, A. Jungbauer, Conformational changes of antibodies upon adsorption onto hydrophobic interaction chromatography surfaces, J. Chromatogr. A 1552 (2018) 60–66, https://doi.org/10.1016/j.chroma.2018.04.009.

[45] H. Song, D. Cabooter, Relevance and assessment of molecular diffusion coefficients in liquid chromatography, Chromatographia 80 (2017) 651–663, https://doi.org/10.1007/s10337-016-3204-z.

[46] K. Kaczmarski, D. Antos, H. Sajonz, P. Sajonz, G. Guiochon, Comparative modeling of breakthrough curves of bovine serum albumin in anion-exchange chromatography. www.elsevier.com/locate/chroma, 2001.

[47] W. Piątkowski, D. Antos, K. Kaczmarski, Modeling of preparative chromatography processes with slow intraparticle mass transport kinetics, J. Chromatogr. A 988 (2003) 219–231, https://doi.org/10.1016/S0021-9673(02)02060-5.

[48] E. Santacesaria, M. Morbidelli, A. Servida, G. Storti, S. Carra, Separation of xylenes on Y zeolites. 2. Breakthrough curves and their interpretation, Ind. Eng. Chem. Process Des. Dev. 21 (3) (1982) 446–451.

[49] M.E. Young, P.A. Carroad, R.L. Bell, Estimation of diffusion coefficients of proteins, Biotechnol. Bioeng. 22 (1980) 947–955, https://doi.org/10.1002/bit.260220504.